Equation of state and effective mass of the unitary Fermi gas in a 1D periodic potential

Gentaro Watanabe,[1,2] Giuliano Orso,[3] Franco Dalfovo,[1] Lev P. Pitaevskii,[1,4] and Sandro Stringari[1]

[1] *CNR INFM-BEC and Department of Physics, University of Trento, 38050 Povo, Italy*
[2] *The Institute of Chemical and Physical Research (RIKEN), 2-1 Hirosawa, Wako, Saitama 351-0198, Japan*
[3] *Laboratoire Physique Théorique et Modèles Statistiques, Université Paris Sud, Bat. 100, 91405 Orsay Cedex, France*
[4] *Kapitza Institute for Physical Problems, 119334 Moscow, Russia*

(Dated: November 20, 2008)

By solving the Bogoliubov – de Gennes equations at zero temperature, we study the effects of a one-dimensional optical lattice on the behavior of a superfluid Fermi gas at unitarity. We show that, due to the lattice, at low densities the gas becomes highly compressible and the effective mass is large, with a consequent significant reduction of the sound velocity. We discuss the role played by the lattice in the formation of molecules and the emergence of two-dimensional effects in the equation of state. Predictions for the density profiles and for the frequency of the collective oscillations in the presence of harmonic trapping are also given.

PACS numbers: 03.75.Ss, 03.75.Kk, 03.75.Lm

arXiv:0806.4713v2 [cond-mat.supr-con] 19 Nov 2008

I. INTRODUCTION

Ultracold gases in optical lattices provide a new frontier of research where many remarkable phenomena can be observed and investigated [1]. By using Feshbach resonances one can tune the interaction between atoms and investigate the BCS-BEC crossover, passing through a resonant regime where the scattering length is very large and the system exhibits universal properties (unitary regime) [2]. First experiments with Fermi superfluids in one-dimensional (1D) optical lattices [3] have focused on the study of the critical velocity along the crossover and revealed that superfluidity is particularly robust at unitarity. The results are in qualitative agreement with the predictions for the Landau critical velocity [4] and for the behavior of the critical current through a single barrier [5].

It is well known that a periodic potential favors the formation of molecules in a two-component Fermi gas (see [6] and references therein), providing an effective shift of the resonance and bound states in the two-body problem even at unitarity. A major problem is to understand the consequences of the molecular formation in the superfluid phase. Moreover, for large laser intensities, the lattice is expected to give rise to 2D effects.

In order to investigate these properties we use a mean-field theory based on the Bogoliubov – de Gennes (BdG) equations [7]. Although approximate, this approach captures basic features along the whole BCS-BEC crossover [8], including the formation of molecules and the most challenging unitary limit where, for uniform 3D configurations, the predictions are in reasonably good agreement with *ab initio* Monte Carlo simulations [9]. The BdG equations apply also to situations where the density varies over distances of the order of the healing length. An important example is given by configurations with quantized vorticity [10]. Furthermore, BdG equations fully account for the modification of the scattering properties of fermions induced by the external confinement as predicted by Petrov *et al.* [11] in the limit of a deep periodic lattice. As a consequence, for example, a tight 1D lattice considerably affects the mean-field superfluid transition temperature, where the BCS order parameter vanishes [12]. Finally, in the case of a deep lattice the BdG theory is expected to approach the 2D mean-field theory of Ref. [13].

In this work we study the unitary regime at zero temperature focusing on the situation in which the lattice potential is relatively weak. In this regime, the tight binding description is not adequate and a full numerical approach based on the BdG equations is called for. By solving the BdG equations, we first calculate the equation of state, the compressibility and the effective mass of the unitary Fermi gas in the lattice. The results are then used to obtain interesting predictions for observable quantities such as the sound velocity, the frequency of collective modes, and the density profile of trapped gases in typical experimental configurations.

II. FORMALISM

At zero temperature, the chemical potential μ of a superfluid Fermi gas in a lattice is given by the derivative of the energy density $e = E/V$ with respect to the average (coarse-grained) density n:

$$\mu = \frac{\partial e(n,P)}{\partial n}\,, \tag{1}$$

where P is the quasi-momentum of the superfluid along the lattice [14]. The compressibility κ and the effective mass m^*, are given by the second derivatives of e with

respect to n and P:

$$\kappa^{-1} = n\frac{\partial^2 e(n,P)}{\partial n^2} = n\frac{\partial \mu(n,P)}{\partial n}\ ; \quad \frac{1}{m^*} = \frac{1}{n}\frac{\partial^2 e(n,P)}{\partial P^2}\,. \tag{2}$$

We calculate these quantities at unitarity for $P = 0$, i.e. for a gas at rest, in the periodic potential

$$V_{\rm ext}(z) = sE_{\rm R}\sin^2 q_{\rm B} z. \tag{3}$$

Here s is the laser intensity, $E_{\rm R} = \hbar^2 q_{\rm B}^2/2m$ is the recoil energy, $q_{\rm B} = \pi/d$ is the Bragg wave vector, d is the lattice constant and m is the atom mass. Then the BdG equations are given by

$$\begin{pmatrix} H'(\mathbf{r}) & \Delta(\mathbf{r}) \\ \Delta^*(\mathbf{r}) & -H'(\mathbf{r}) \end{pmatrix} \begin{pmatrix} u_i(\mathbf{r}) \\ v_i(\mathbf{r}) \end{pmatrix} = \epsilon_i \begin{pmatrix} u_i(\mathbf{r}) \\ v_i(\mathbf{r}) \end{pmatrix}\ , \tag{4}$$

where $H'(\mathbf{r}) = -\hbar^2\nabla^2/2m + V_{\rm ext} - \mu$. The order parameter $\Delta(\mathbf{r})$ and the chemical potential μ, appearing in Eq. (4), are variational parameters determined from the self-consistency relation

$$\Delta(\mathbf{r}) = -g\sum_i u_i(\mathbf{r})v_i^*(\mathbf{r}), \tag{5}$$

together with the constraint $n = (2/V)\sum_i \int |v_i(\mathbf{r})|^2\, d\mathbf{r}$, enforcing conservation of the average density n. In Eq. (5), g is the coupling constant for the contact interaction and the BdG eigenfunctions obey the normalization condition $\int d\mathbf{r}\,[u_i^*(\mathbf{r})u_j(\mathbf{r}) + v_i^*(\mathbf{r})v_j(\mathbf{r})] = \delta_{i,j}$.

For contact interactions, the right hand side of Eq. (5) is ultraviolet divergent and must be cured by the pseudopotential method. A standard procedure consists of introducing a cut-off energy $E_{\rm C}$ in the sums over the BdG eigenstates and of replacing the bare coupling constant by the s-wave scattering length $a_{\rm s}$ through the relation $(k_{\rm F}a_{\rm s})^{-1} = 8\pi E_{\rm F}/(gk_{\rm F}^3) + (2/\pi)\sqrt{E_{\rm C}/E_{\rm F}}$, where $k_F = (3\pi^2 n)^{1/3}$ and $E_{\rm F} = \hbar^2 k_F^2/(2m)$ are the Fermi wave vector and energy, respectively, of a uniform noninteracting Fermi gas with density n. An alternative regularization scheme is the one proposed in Refs. [15, 16]. This method exploits directly the short distance behavior of the single-particle Green's function and is efficient even in the presence of a tight confinement. Both procedures give identical results provided $E_{\rm C}$ is large enough.

In the presence of a supercurrent with wave vector $Q = P/\hbar$ moving along the lattice, one can write the order parameter in the form $\Delta(\mathbf{r}) = e^{i2Qz}\tilde{\Delta}(z)$, where $\tilde{\Delta}(z)$ is a complex function with period d. Therefore, from Eq. (5), we see that the eigenfunctions of Eq. (4) must have the Bloch form $u_i(\mathbf{r}) = \tilde{u}_i(z)e^{iQz}e^{i\mathbf{k}\cdot\mathbf{r}}$ and $v_i(\mathbf{r}) = \tilde{v}_i(z)e^{-iQz}e^{i\mathbf{k}\cdot\mathbf{r}}$, where k_z lies in the first Brillouin zone and $\tilde{u}_i$ and $\tilde{v}_i$ are periodic in z with period d. This transformation reduces Eq. (4) to the BdG equations for $\tilde{u}_i$ and $\tilde{v}_i$ as

$$\begin{pmatrix} \tilde{H}'_Q(z) & \tilde{\Delta}(z) \\ \tilde{\Delta}^*(z) & -\tilde{H}'_{-Q}(z) \end{pmatrix} \begin{pmatrix} \tilde{u}_i(z) \\ \tilde{v}_i(z) \end{pmatrix} = \epsilon_i \begin{pmatrix} \tilde{u}_i(z) \\ \tilde{v}_i(z) \end{pmatrix}\ , \tag{6}$$

where

$$\tilde{H}'_Q(z) \equiv \frac{\hbar^2}{2m}\left[k_x^2 + k_y^2 + (-i\partial_z + Q + k_z)^2\right] + V_{\rm ext}(z) - \mu\,. \tag{7}$$

From now on, the label i represents the wave vector $\mathbf{k}$ as well as the band index.

From the solution of the BdG equations, we can directly calculate μ and κ [see Eqs. (1) and (2)], while m^* is obtained from the energy density $e(n,P)$ [7]

$$e = \int d\mathbf{r}\left[\sum_i 2(\mu - \epsilon_i)|\tilde{v}_i(z)|^2 + \sum_i \tilde{\Delta}^*(z)\tilde{u}_i(z)\tilde{v}_i^*(z)\right]. \tag{8}$$

Note that in the rhs of Eq. (8) both contributions are separately divergent but the sum is finite, as one can easily check for the uniform case ($s = 0$).

III. RESULTS

A first important remark concerns the low density limit of μ and m^* whose values are found in perfect agreement with the results of the exact solution of the two-body problem [6]. This proves that the BdG theory correctly accounts for the deep modifications of the atomic scattering properties induced by the external confinement which gives rise to bound molecules even at unitarity.

Our results for the density dependence of κ^{-1} and m^* at unitarity are shown in Figs. 1(a) and 1(b). They are plotted for $s = 1$, 2.5, and 5, as functions of $E_{\rm F}/E_{\rm R} = (k_{\rm F}d/\pi)^2$. The solid, dashed and dashed-dotted lines correspond to the values obtained with the regularization scheme of Ref. [16] and choosing the cut-off energy large enough to ensure convergence within 1-2% [17]. In order to appreciate the role of the cut-off energy, we also plot the results obtained using the standard regularization procedure with $E_{\rm C} = 100E_{\rm F}$ (points). The results agree within 10-15%, the accuracy being worse in the small density regime $E_{\rm F} \ll E_{\rm R}$.

In the absence of the lattice ($s = 0$) the results take a universal behavior at unitarity: the only relevant length being the interparticle distance fixed by $k_{\rm F}$. Due to translational invariance, one can write $e(n,P) = e(n,0) + nP^2/2m$ so that $m^* = m$. Furthermore, the energy density at $P = 0$ can be written as $e(n,0) = (1+\beta)e^0(n,0)$, where $e^0(n,0) \equiv (3/5)nE_{\rm F}$ is the ideal Fermi gas value and β is the dimensionless universal parameter accounting for the interactions in uniform gas. The BdG equations predict $\beta \simeq -0.41$ to be compared with the Monte Carlo result $\beta \simeq -0.58$ [9].

A. Unitary Fermi gas in a lattice

1. Equation of State

New features appear when s increases. Let us first discuss the behavior of the equation of state. At small

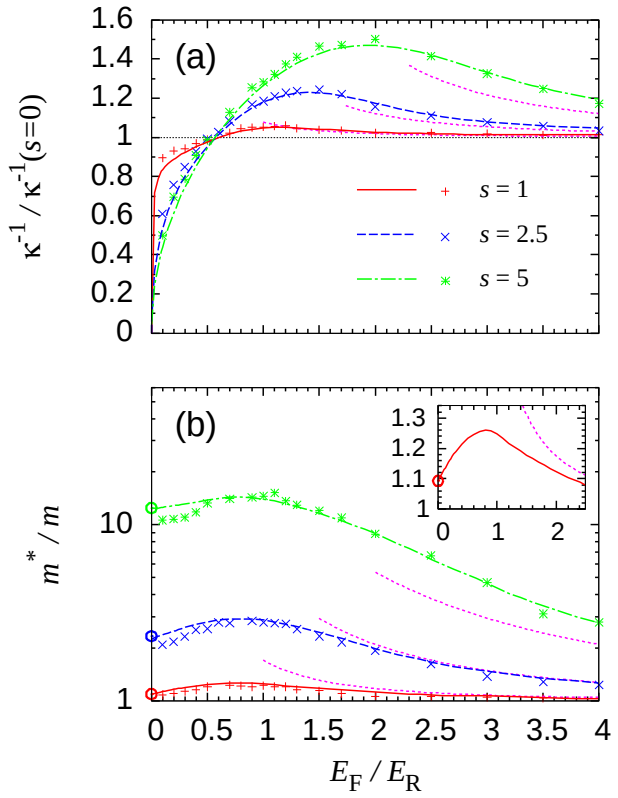

FIG. 1: (Color online) Inverse compressibility κ^{-1}, and effective mass m^* of the unitary Fermi gas for $s = 1$ (red), 2.5 (blue), and 5 (green). Lines are convergent results obtained by the regularization scheme of Ref. [16]. Points are obtained by means of the standard regularization scheme with $E_C = 100E_F$. Asymptotic expressions (9) and (10) are shown by the dotted lines. Open circles in panel (b) show m^* obtained in Ref. [6]. The $s = 1$ results for m^* are also shown in the inset in the linear scale.

densities ($E_F/E_R \ll 1$) we find that the lattice causes a linear density dependence of the chemical potential [see inset of Fig. 4] and a strong suppression of κ^{-1} with respect to the uniform value [see Fig. 1(a)]. These results are consistent with the tendency of the lattice to favor the formation of molecules. The size of these molecules is fixed by the values of s and d so that, in the limit of a dilute gas ($k_F d \ll 1$), the interparticle distance can be larger than the molecular size. In this limit, the BdG equation describes the formation of a molecular gas which gives rise to Bose-Einstein condensation; the equation of state is given by the Bogoliubov theory and κ^{-1} is expected to be linear in the density, yielding $\kappa^{-1}/\kappa^{-1}(s = 0) \propto n^{1/3} \to 0$. For $s \gg 1$ the chemical potential remains almost linear in density even at relatively large densities, due to 2D effects caused by the bandgap in the longitudinal motion (see discussion below). At even higher densities, one eventually recovers the behavior of a uniform gas since the lattice only provides a small perturbation. By using an hydrodynamic approach and expanding in the small parameter sE_R/E_F, we find [18]

$$\kappa^{-1} \simeq \frac{2}{3}(1+\beta)E_F\left[1+\frac{1}{32}(1+\beta)^{-2}\left(\frac{sE_R}{E_F}\right)^2\right] + O\left[(sE_R/E_F)^4\right] \quad (9)$$

This is shown by dotted lines in Fig. 1(a).

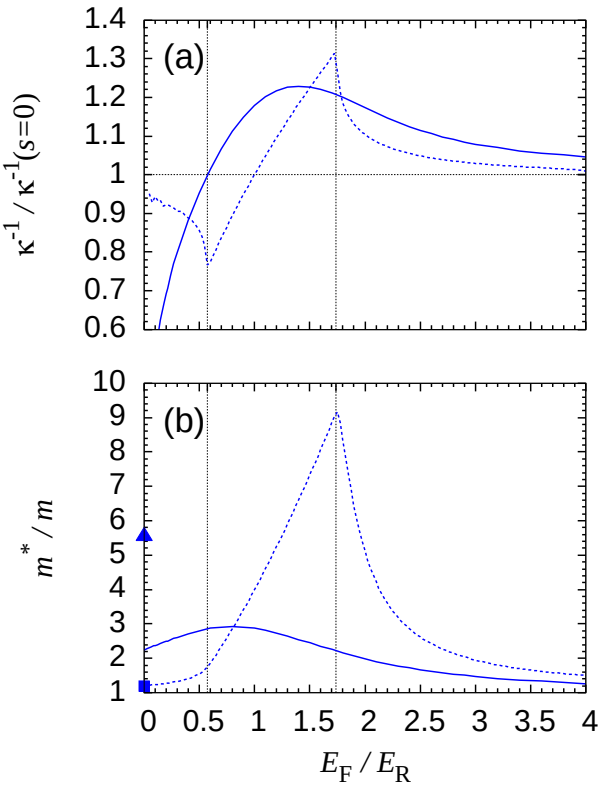

FIG. 2: (Color online) Comparison between the unitary Fermi gas (solid lines) and the ideal Fermi gas (dashed lines) in the same optical lattice with $s = 2.5$. The region between the two vertical lines represents the range where the chemical potential of the ideal gas lies in the bandgap above the lowest Bloch band. In panel (b), the square at $m^*/m = 1.20$ shows the value of the effective mass of a single atom with mass m in the same lattice, while the triangle at $m^*/m = 5.53$ shows that of a point-like molecule with mass $2m$.

2. *Effective Mass*

The formation of molecules has important consequences also for m^*. Due to this effect, at low densities, the enhancement of m^* caused by lattice is much more dramatic in the unitary Fermi gas compared to the ideal Fermi gas (or, equivalently to m^* in the BCS limit) and to the gas of bosons with the same mass m (see Fig. 4 in Ref. [19]). We also note that, for a given s, the value of m^* at $E_F \to 0$ lies between the value of m^* for a single atom of mass m in the same lattice [square in the

vertical axis of Figs. 2(b)] and the value of m^* calculated for a point-like molecule of mass $2m$ (triangle). As E_F/E_R increases, the effective mass exhibits a maximum at $E_F/E_R \sim 1$, then it decreases towards the bare mass, $m^* = m$. The same hydrodynamic argument used for κ^{-1} also explains the behavior of the effective mass for small sE_R/E_F:

$$\frac{m^*}{m} \simeq 1+\frac{9}{32}(1+\beta)^{-2}\left(\frac{sE_R}{E_F}\right)^2+O\left[(sE_R/E_F)^4\right] , \quad (10)$$

showing that the effect of the lattice is stronger for m^* than for κ^{-1}. It is worth comparing the results with the case of bosonic atoms, where m^* decreases monotonically with increasing density since the interaction broadens the condensate wave function and favors the tunneling [19].

3. Comparison with the Ideal Fermi Gas

The occurrence of a maximum in the curves for both κ^{-1} and m^* can be interpreted as an effect of the energy gap in the longitudinal motion, which opens at $q = q_B$. An instructive comparison can be made with an ideal Fermi gas in the same lattice, where the effects of the bandgap are more evident due to the sharper Fermi surface. In Fig. 2 one sees that the ideal gas curves have two cusps. They occur precisely when μ coincides with the top of the lowest band and the bottom of the first excited band at $q = q_B$, respectively. In between, as E_F/E_R increases, only the transverse modes are available and the system behaves effectively like a 2D system, the longitudinal degree of freedom simply giving a constant contribution to κ^{-1} and m^*. Consequently, κ^{-1} and m^* are proportional to the average density in this region (see Eqs. (10) and (11) in Ref. [20]) and one finds the power laws $\kappa^{-1}/\kappa^{-1}(s=0) \propto E_F^{1/2}$ and $m^* \propto E_F^{3/2}$. The interval where this 2D behavior takes place becomes wider as s increases, since the bandgap increases with s. By comparing the ideal and unitary Fermi gases, we see that the interaction significantly smears the effect of the gap as a result of a much broader Fermi surface. Especially the maximum values of m^* are drastically reduced. Note also that the molecular-like pair correlations, which are responsible for the low density behavior of κ^{-1} and m^*, are absent in the ideal Fermi gas.

4. Sound Velocity

Our results for κ^{-1} and m^* can be used to calculate the sound velocity $c_s = \sqrt{\kappa^{-1}/m^*}$, which is given in Fig. 3. One can see a significant reduction of c_s compared to the uniform system. Except for very low densities, the sound velocity varies rather smoothly with the density. This makes it possible to provide an estimate the change of c_s induced by the lattice even for harmonically trapped gases, where the coarse-grained density is not uniform.

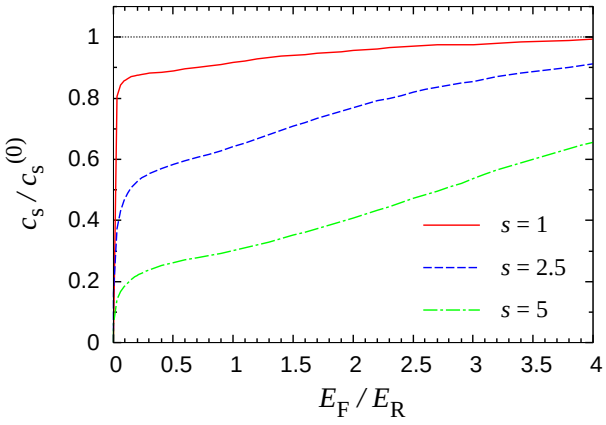

FIG. 3: (Color online) Sound velocity c_s in units of the sound velocity $c_s^{(0)} = [(2/3)(1+\beta)E_F/m]^{1/2}$ for the uniform system. As in Fig. 1, red, blue and green lines correspond to $s = 1, 2.5$, and 5, respectively.

Notice that the propagation of sound is a direct consequence of superfluidity and, in the presence of tight lattices, can be regarded as a Josephson effect, where the gas tunnels in a coherent way through the barriers produced by the lattice.

B. Unitary Fermi gas in a lattice + trap

1. Density Profile

We can also provide useful predictions for the density profile and for the collective motion of a trapped gas, when a harmonic confinement is added to the periodic potential. The coarse-grained density profile, $n(z)$, is easily calculated using the local density approximation (LDA) for μ. Figure 4 clearly shows that, for $s = 5$, the profile takes the form of an inverted parabola, reflecting the linear density dependence of the chemical potential (see inset). In this calculation, we set $\omega_\perp = \omega_z$, where $\omega_\perp$ and ω_z are the transverse and longitudinal trapping frequencies, $\hbar\omega_z/E_R = 0.01$, and the number of particles $N = 10^6$; these parameters are close to the experimental ones in Ref. [3].

The accurate measurement of the density profile in the presence of harmonic trapping can actually give direct information on the compressibility of the gas. In fact, within the range of validity of LDA, the two quantities obey a simple relationship which, for isotropic traps, is

$$\frac{\partial n}{\partial r} = -m\omega^2 r\left(\frac{\partial \mu}{\partial n}\right)^{-1} . \quad (11)$$

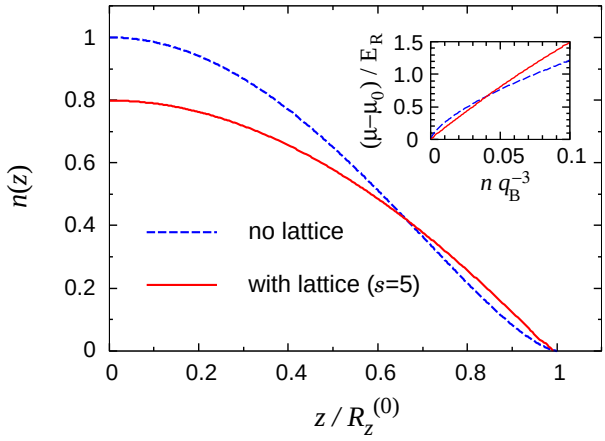

FIG. 4: (Color online) Coarse-grained density profiles of a trapped gas, $n(r_\perp = 0, z)$ for $s = 0$ and 5 in units of the central density $n(0) = 0.0869 q_B^3$ calculated for $s = 0$ (this local density corresponds to $E_F/E_R = 1.88$). The quantity $R_z^{(0)}$ is the axial Thomas-Fermi radius for $s = 0$. The inset shows the density dependence of the chemical potential. The parameters of the trap are given in the text.

2. *Collective Modes*

The collective modes can be studied by solving the hydrodynamic equations, where the periodic potential is included through its effects on the equation of state $\mu(n)$ and on the effective mass which determines the current in the longitudinal direction [21]. While the frequency of the dipole (center-of-mass) oscillation along the transverse direction is not affected by the lattice, a useful estimate for the dipole frequency in the z-direction can be obtained using a sum rule approach based on the calculation of the energy weighted and inverse energy weighted moments of the dipole strength within the hydrodynamic theory [20]. This approach yields the result $\omega_D = \omega_z (m/\overline{m^*})^{1/2}$ where

$$\frac{1}{\overline{m^*}} = \frac{1}{N} \int d\mathbf{r} \, \frac{n(\mathbf{r})}{m^*[n(\mathbf{r})]} \, . \qquad (12)$$

Even without calculating $n(\mathbf{r})$, we can easily estimate lower and upper bounds for the frequency by replacing $\overline{m^*}$ with the maximum and minimum values of m^* as a function of n as one moves from the center to the border of the atomic cloud. For clouds whose maximum density is such that $E_F/E_R \lesssim 1.5$ the minimum value corresponds to the low density $E_F/E_R \to 0$ limit, while the maximum corresponds to the absolute maximum of the curves in Fig. 1(b). In this way we obtain the estimate $0.89 \leq \omega_D/\omega_z \leq 0.96$ for $s = 1$, $0.59 \leq \omega_D/\omega_z \leq 0.66$ for $s = 2.5$, and $0.26 \leq \omega_D/\omega_z \leq 0.28$ for $s = 5$.

Finally, the effects of the lattice on the equation of states can be observed also by studying the compression modes. For example, taking the cigar shape geometry $\omega_z \ll \omega_\perp$, the frequency of the radial breathing mode is unaffected by m^*. In the regime where the chemical potential is linear in the density (see inset of Fig. 4) the collective frequency approaches the value $\omega = 2\omega_\perp$, while its value is $\sqrt{10/3}\omega_\perp$ in the absence of the lattice. The transition between the two different regimes is similar to the one recently investigated by varying the scattering length on the BEC side of the resonance in the absence of periodic potentials (see, e.g., [2]).

IV. CONCLUSION

In this work we have shown that the inclusion of a 1D optical lattice, by favoring the formation of molecular configurations and by inducing a band structure in the quasiparticle spectrum, has profound consequences on the thermodynamic quantities, the density profile, and the collective oscillations of the unitary Fermi gas. Our calculations can be naturally extended to the case of finite quasi-momenta, where energetic and dynamic instabilities are expected to impose some limits to the superfluid motion. Further investigations of the 2D nature of the many-body system achievable with large laser intensities are also in progress.

Acknowledgments

We thank M. Antezza, G. Bruun, E. Furlan, S. Giorgini, Y. Ohashi, and M. Urban for fruitful discussions. G. O. is supported by the Marie Curie Fellowship under contract n. EDUG-038970. This work has been supported by MIUR and by Fermix-Euroquam.

[1] I. Bloch, J. Dalibard, and W. Zwerger, Rev. Mod. Phys. **80**, 885 (2008).
[2] S. Giorgini, L. P. Pitaevskii, and S. Stringari, Rev. Mod. Phys. **80**, 1215 (2008).
[3] D. E. Miller, J. K. Chin, C. A. Stan, Y. Liu, W. Setiawan, C. Sanner, and W. Ketterle, Phys. Rev. Lett. **99**, 070402 (2007).
[4] R. Combescot, M. Yu. Kagan, and S. Stringari, Phys. Rev. A **74**, 042717 (2006).
[5] A. Spuntarelli, P. Pieri, and G. C. Strinati, Phys. Rev. Lett. **99**, 040401 (2007).
[6] G. Orso, L. P. Pitaevskii, S. Stringari, and M. Wouters, Phys. Rev. Lett. **95**, 060402 (2005).
[7] P. G. de Gennes, *Superconductivity of Metals and Alloys*, (Benjamin, New York, 1966), Chap. 5, pp. 137–170.
[8] M. Randeria, in *Bose Einstein Condensation*, edited by

A. Griffin, D. Snoke, and S. Stringari (Cambridge, Cambridge, England, 1995), Chap. 15, pp. 355–392.
[9] J. Carlson, S.-Y. Chang, V. R. Pandharipande, and K. E. Schmidt, Phys. Rev. Lett. **91**, 050401 (2003); G. E. Astrakharchik, J. Boronat, J. Casulleras, and S. Giorgini, *ibid.* **93**, 200404 (2004).
[10] R. Sensarma, M. Randeria, and T.-L. Ho, Phys. Rev. Lett. **96**, 090403 (2006).
[11] D. S. Petrov, M. Holzmann, and G. V. Shlyapnikov, Phys. Rev. Lett. **84**, 2551 (2000).
[12] G. Orso and G. V. Shlyapnikov, Phys. Rev. Lett. **95**, 260402 (2005).
[13] M. Randeria, J.-M. Duan, and L.-Y. Shieh, Phys. Rev. Lett. **62**, 981 (1989).
[14] The knowledge of the P-dependence of the energy density also permits to calculate the current $I(n,P) = \partial e(n,P)/\partial P$ carried by the system in the presence of the lattice.
[15] G. Bruun, Y. Castin, R. Dum, and K. Burnett, Eur. Phys. J. D **7**, 433 (1999).
[16] A. Bulgac and Y. Yu, Phys. Rev. Lett. **88**, 042504 (2002).
[17] In practice, we include more than 20 single-particle Bloch bands in these calculations.
[18] In the limit of $E_{\rm F} \gg E_{\rm R}$, the length scale of the density variation $\sim d$ is much larger than the coherence length $\xi \sim k_{\rm F}^{-1}$ (at unitarity) since $(d/\xi)^2 \sim (k_{\rm F}/q_{\rm B})^2 \gg 1$, which validates the hydrodynamic theory.
[19] M. Krämer, C. Menotti, L. Pitaevskii, and S. Stringari, Eur. Phys. J. D **27**, 247 (2003).
[20] L. P. Pitaevskii, S. Stringari, and G. Orso, Phys. Rev. A **71**, 053602 (2005).
[21] L. P. Pitaevskii and S. Stringari, *Bose-Einstein Condensation* (Clarendon, Oxford, 2003), Chap. 16, pp. 303–322.